J|A|C|S ARTICLES

Published on Web 07/02/2009

Permeation of Membranes by Ribose and Its Diastereomers

Chenyu Wei[†,§] and Andrew Pohorille*[,‡,§]

NASA Ames Research Center, Mail Stops 229-1 and 239-4, Moffett Field, California 94035, and Department of Pharmaceutical Chemistry, University of California, San Francisco, San Francisco, California 94143-2280

Received April 3, 2009; E-mail: chenyu.wei@nasa.gov; pohorill@raphael.arc.nasa.gov

Abstract: It was recently found that ribose permeates membranes an order of magnitude faster than its diastereomers arabinose and xylose (Sacerdote, M. G.; Szostak, J. W. *Proc. Natl. Acad. Sci. U.S.A.* **2005**, *102*, 6004). On this basis it was hypothesized that differences in membrane permeability to aldopentoses provide a mechanism for preferential delivery of ribose to primitive cells for subsequent selective incorporation into nucleotides and their polymers. However, the origins of these unusually large differences have not been well understood. We address this issue in molecular dynamics simulations combined with free energy calculations. It is found that the free energy of transferring ribose from water to the bilayer is lower by 1.5−2 kcal/mol than the barrier for transferring the other two aldopentoses. The calculated and measured permeability coefficients are in excellent agreement. The sugar structures that permeate the membrane are β-pyranoses, with a possible contribution of the α-anomer for arabinose. The furanoid form of ribose is not substantially involved in permeation, even though it is non-negligibly populated in aqueous solution. The differences in free energy of transfer between ribose and arabinose or xylose are attributed, at least in part, to stronger highly cooperative, intramolecular interactions between consecutive exocyclic hydroxyl groups, which are stable in nonpolar media but rare in water. Water/hexadecane partition coefficients of the sugars obtained from separate molecular dynamics simulations correlate with the calculated permeability coefficients, in qualitative agreement with the Overton rule. The relevance of our calculations to understanding the origins of life is discussed.

Introduction

Permeation of molecules through membranes is a fundamental process in biological systems, which not only involves mass and signal transfers between the interior of a contemporary cell and its environment but also was of crucial importance in the origin of life. In the absence of complex protein transporters, nutrients and building blocks of biopolymers must have been able to permeate membranes at sufficient rates to support primordial metabolism and cellular reproduction. From this perspective one class of solutes that is of special interest are monosaccharides, which serve not only as nutritional molecules but also as building blocks for information molecules. In particular, ribose is a part of the RNA backbone, but RNA analogues containing a number of other sugars have also been shown to form stable duplexes.[1,2] Why, among these possibilities, ribose (and subsequently, deoxyribose) was selected for the backbone of information polymers is still poorly understood.

Recent experiments by Sacerdote and Szostak[3] shed new light on this problem. In these experiments, it was shown that ribose permeates membranes markedly faster than its diastereomers arabinose, xylose, and lyxose. This unusual phenomenon has been observed for bilayers of both phospholipids, such as 1-palmitoyl-2-oleoyl-*sn*-glycero-3-phosphocholine (POPC), and much simpler membranes built of fatty acids, such as myrystoleic and oleic acids. Although the absolute values of the permeability coefficients depend on membrane composition, they are consistently higher for ribose than for arabinose or xylose by approximately an order of magnitude. Sacerdote and Szostok hypothesized that ribose might have been favored in RNA over other aldopentoses because it could have been supplied more quickly to primitive cells and would therefore have been more readily available for synthesis of nucleotides and their subsequent polymerization.[3] This is consistent with other studies indicating that passive uptake of organic material might have been a rate-limiting step in a number of protocellular processes, such as template-directed replication of RNA[4−7] or protein synthesis.[8]

The reasons for preferential permeation of ribose are not clear. The conventional framework for analyzing this problem is based on the solubility-diffusion model.[9,10] In its most common

[†] NASA Ames Research Center, Mail Stop 229-1.
[‡] NASA Ames Research Center, Mail Stop 239-4.
[§] University of California San Francisco.

(1) Beier, M.; Reck, F.; Wagner, T.; Krishnamurthy, R.; Eschenmoser, A. *Science* **1999**, *283*, 699.
(2) Schoning, K.-U.; Scholz, P.; Wu, X.; Guntha, S.; Delgado, G.; Krishnamurthy, R.; Eschenmoser, A. *Helv. Chim. Acta* **2002**, *85*, 4111.
(3) Sacerdote, M. G.; Szostak, J. W. *Proc. Nat. Acad. Sci. U.S.A.* **2005**, *102*, 6004.
(4) Chakrabarti, A. C.; Breaker, R. R.; Joyce, G. F.; Deamer, D. W. *J. Mol. Evol.* **1994**, *39*, 555.
(5) Monnard, P. A.; Deamer, D. W. *Origins Life Evol. Biospheres* **2001**, *31*, 147.
(6) Monnard, P. A.; Luptak, A.; Deamer, D. W. *Philos. Trans. R. Soc., B* **2007**, *362*, 1741.
(7) Mansy, S. S.; Schrum, J. P.; Krishnamurthy, M.; Tobé, S.; Treco, D. A.; Szostak, J. W. *Nature* **2008**, *454*, 122.
(8) Chakrabarti, A. C.; Deamer, D. W. *J. Mol. Evol.* **1994**, *39*, 1.

application, it is assumed that solute permeation through a membrane consists of two steps: transfer from the aqueous solution to the bilayer and diffusion across the membrane. The bilayer is treated as a homogeneous, isotropic lamella, sharply separated from the aqueous medium. Under these assumptions the diffusion coefficient is the same everywhere in the membrane. If one further assumes that the diffusion coefficient is approximately the same for all solutes of interest, membrane permeability depends only on the partition coefficient between water and membrane, which can be approximated as partition coefficient between water and a bulk nonpolar phase. This yields the Overton rule, which states that the permeability of a membrane to different solutes correlates with the water−octanol partition coefficients of the solutes.[11] Subsequently it was found that membrane permeabilities correlate even better with partition coefficients between water and hexadecane or 1,9-decadiene.[12,13]

Using a simple predictive model, Sacerdote and Szostak found that the water−octanol partition coefficients for all aldopentoses were nearly identical.[3] On this basis it was concluded that the framework of the solubility-diffusion model was inadequate to explain different permeation rates of these compounds and other effects must be at play. It was conjectured that the furanose form of ribose, which is populated in water significantly more than for other aldopentoses, might permeate faster than the pyranose form or that ribose might permeate membranes as α-pyranose dimers.

There is also another possibility. Predicted partition coefficients for closely related sugars are inaccurate because they do not incorporate information about solvent-mediated changes in molecular structure of the solute. To test this possibility we carry out molecular dynamics (MD) simulations aimed at calculating permeability of the POPC membrane to ribose, arabinose, and xylose. The permeabilities are obtained using the conceptual framework of the solubility-diffusion model, but its most questionable approximations, such as homogeneity of the membrane and the assumption that the diffusion coefficient is constant everywhere in the bilayer, are not required. In addition, analysis of the results might reveal which factors are responsible for increased permeation of ribose compared to the other two aldopentoses. POPC has been selected as the membrane-forming material because the area coverage per headgroup for these phospholipids has been measured[14] and the structure of the bilayer has already been studied in computer simulations.[15−20]

As the first step, we perform MD simulations in which the three aldopentoses are transferred from water to hexadecane and calculate their partition coefficients between the two phases. Dynamics of hexadecane in the bulk and phospholipid chains inside the bilayer, which are important for solute partition and permeation, have been shown to be similar.[21] To account for structural flexibility of cyclic sugars,[22] we consider several constitutional isomers and conformers that might be populated in polar or nonpolar environments. The water−hexadecane simulations serve two purposes. We test whether partition coefficients of aldopentoses correlate with membrane permeabilities, as postulated by the Overton rule. We also use the results of these simulations to select a small subset of sugar structures that are most likely to have the highest rates of permeation through membranes. Only these structures are considered in subsequent simulations of the water−POPC systems. This greatly reduces the computational effort required to calculate the permeabilities.

Methods

Molecular Dynamics Simulation. All MD simulations reported here were carried out using NAMD.[23] CHARMM potentials were used to describe the phospholipids forming the membrane[24] and carbohydrates.[25,26] Water was represented as the TIP3 model. The simulations involved a sugar molecule in either the water−hexadecane or the water−POPC system. The water−hexadecane system consisted of lamellae formed by 66 hexadecane molecules and 988 water molecules in direct contact, the thicknesses of which were 42 and 30 Å, respectively. The x, y, and z dimensions of the simulation box were ∼30 Å × 30 Å × 72 Å, with the z coordinate perpendicular to the interface. Periodic boundary conditions were applied in all three spatial directions. To prepare the hexadecane phase, individual chains were relaxed using Monte Carlo simulations. Density of the bulk hexadecane at 298 K was equal to 770 kg/m^3, in agreement with the experimental value of 773 kg/m^3 at the same temperature.[27] The *NPT* ensemble at pressure $P = 1$ atm was used to simulate the system. During equilibration, the temperature was raised to the target value of 310 K. The water−POPC system consisted of a POPC bilayer approximately 30 Å thick built of 26 phospholipid molecules and a water lamella consisting of 1858 molecules. They were enclosed in a periodic box, the dimensions of which were ∼30 Å × 30 Å × 62 Å. The x,y dimensions of this system would be rather small for simulating proteins in membranes but are sufficient for studying permeation of solutes that are only a few angstroms across. For this system, the temperature was 303 K, the pressure was 1 atm in the direction perpendicular to the water−membrane interface, and the surface area was kept constant at 68.3 Å^2 per lipid molecule, which is the value measured in a recent X-ray scattering experiment.[14] Before the production simulations, the system was equilibrated for 5 ns.

A time step of 1 fs was used in all simulations. The temperature was kept constant by applying the Langevin friction force scheme (5 ps^{-1} was used for the damping coefficient). Particle Mesh Ewald scheme was used to calculate long-range electrostatic interactions (using a grid of 32 × 32 × 128 points for the hexadecane−water system and 32 × 32 × 64 points for the POPC−water system), and van der Waals interactions were cut off at 13.5 Å.

Free Energy Calculations: Adaptive Biasing Force Method. The free energy profile, $A(z)$, for transferring a sugar molecule across the water−hexadecane or water−POPC interface was

(9) Hanai, T.; Dayton, D. A. *J. Theor. Biol.* **1966**, *11*, 1370.
(10) Finkelstein, A.; Cass, A. E. *Nature* **1967**, *216*, 717.
(11) Overton, E. *Vierteljahrsschr. Naturforsch. Ges. Zurich* **1899**, *44*, 88.
(12) Walter, A.; Gutknecht, J. *J. Membr. Biol.* **1986**, *90*, 207.
(13) Xiang, T. X.; Anderson, B. D. *J. Membr. Biol.* **1940**, *140*, 111.
(14) Kucerka, N.; Tristram-Nagle, S.; Nagle, J. F. *J. Membr. Biol.* **2005**, *208*, 193.
(15) Armen, R. S.; Uitto, O. D.; Feller, S. E. *Biophys. J.* **1998**, *75*, 734.
(16) Ceccarelli, M.; Marchi, M. *Biochimie* **1998**, *80*, 415.
(17) Chiu, S. W.; Jakobsson, E.; Subramaniam, S.; Scott, H. L. *Biophys. J.* **1999**, *77*, 2462.
(18) Jójárt, B.; Martinek, T. A. *J. Comput. Chem.* **2007**, *28*, 2051.
(19) Leekumjorn, S.; Sum, A. K. *J. Phys. Chem. B* **2007**, *111*, 6026.
(20) Taylor, J.; Whiteford, N. E.; Bradley, G.; Watson, G. W. *Biochim. Biophys. Acta* **2009**, *1788*, 638.
(21) Venable, R. M.; Zhang, Y.; Hardy, B. J.; Pastor, R. W. *Science* **1993**, *262*, 223.
(22) Rao, V. S. R.; Qasba, P. K.; Balaji, P. V.; Chandrasekaran, R. *Conformation of Carbohydrates*; Harwood Academic Publishers: Amsterdam, 1998.
(23) Phillips, J. C.; Braun, R.; Wang, W.; Gumbart, J.; Tajkhorshid, E.; Villa, E.; Chipot, C.; Skeel, R. D.; Kale, L.; Schulten, K. *J. Comput. Chem.* **2005**, *26*, 1781.
(24) MacKerell, A. D., Jr. *J. Phys. Chem. B* **1998**, *102*, 3586.
(25) Ha, S. N.; Giammona, A; Field, M.; Brady, J. W. *Carbohydr. Res.* **1988**, *180*, 207.
(26) Schmidt, R. K.; Karplus, M.; Brady, J. W. *J. Am. Chem. Soc.* **1996**, *118*, 541.
(27) Dymond, J. H.; Harris, K. R. *Mol. Phys.* **1992**, *75*, 461.

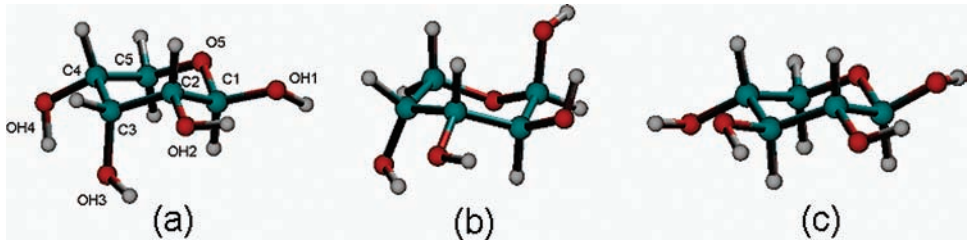

Figure 1. Snapshot of sugar molecules using a ball-and-stick representation: (a) β-ribopyranose ($^4C_1$ chair); (b) β-arabinopyranose ($^1C_4$ chair); (c) β-xylopyranose ($^4C_1$ chair). Carbon, oxygen, and hydrogen atoms are blue, red, and white, respectively.

calculated as a function of an order parameter ("reaction coordinate"), z, defined as the z component of the distance between the center of mass of the sugar molecule and the center of mass of either the hexadecane lamella or the POPC bilayer. To obtain $A(z)$ we used the NAMD implementation[28] of the Adaptive Biasing Force (ABF) method.[29,30] This thermodynamic integration approach guarantees nearly optimal efficiency of calculating free energy along a generalized coordinate or on a low dimensional manifold. It consists of two steps: (1) extracting the thermodynamic force along specified generalized coordinates in unconstrained dynamics, and (2) subtracting the position-dependent average force from the instantaneous force in an adaptive manner. As a result, the specified coordinates are sampled uniformly. To obtain the free energy changes, the calculated average force is integrated along the coordinates of interest. The high efficiency of this approach is due to the fact that forces, in contrast to probabilities, are local properties and, therefore, can be efficiently updated without exploring the reminder of the configurational space. Recently, the ABF method has been successfully applied by several authors to such challenging problems as protein unfolding, protein−protein associations, and solute transport across membrane channels.[31−36]

For the water−hexadecane systems, free energy calculations were divided into four regions ("windows") along z, each 6 Å wide. Harmonic restraints at the edges of the window kept the solute in the prescribed region. ABF simulations 7−10 ns long were performed in each window. The simulations covered a region of z 24 Å wide, which ranged from bulk water to bulk hexadecane. For the water−POPC system, four similar ABF windows were used to cover a range of z that was 25 Å wide and extended from bulk water to the center of the POPC membrane. ABF simulations 8−9 ns long were performed in every window. To achieve higher statistical accuracy near the center of the bilayer (-9 Å $< z < 0$ Å), we extended simulations in this region to 17−25 ns.

The upper limit of the standard error in ABF calculation, $\mathrm{SD}[\Delta A^{(\mathrm{ABF})}]$, for the free energy difference, $\Delta A^{(\mathrm{ABF})}$, between points ξ_a and ξ_b along a reaction coordinate, ξ, can be estimated as[37]

$$\mathrm{SD}[\Delta A^{(\mathrm{ABF})}] \approx (\xi_b - \xi_a)\frac{\sigma}{K^{1/2}}(1 + 2\kappa)^{1/2} \qquad (1)$$

where σ^2 is the variance of thermodynamic force along ξ, K is the total number of force values computed in the entire simulation, and κ is the correlation length for the series of calculated forces.[38]

Table 1. Populations of Different Forms of Aldopentoses in Aqueous Solution[40]

	pyranose		furanose	
	α-form (%)	β-form (%)	α-form (%)	β-form (%)
D-ribose	21.5	58.5	6.5	13.5
D-xylose	36.5	63.0	0	0
D-arabinose	60.0	35.5	2.5	2

Conformations of Aldopentoses. Aldopentoses and closely related aldohexoses can adopt a number of structures.[22] The sugar ring can be either five-membered (furanose) or six-membered (pyranose). In each case, the hydroxyl group that is attached to the C_1 carbon atom can be pointing either up or down relative to the plane of the ring structure, and the molecule is labeled α or β, respectively. The up/down notation for the OH group is defined according to Haworth projection formulas.[39] Both furanose and pyranose rings are puckered and can exist in several conformations. Pyranose usually adopts the $^4C_1$ or $^1C_4$ chair conformations, although other conformations, such as boats or skew-boats, are also possible.[22] They have not been considered in this study because they are less stable than the chair conformations. We only investigate D-sugars to be consistent with the experiment[3] and will omit this notation for simplicity. Finally, the hydroxyl groups attached to the sugar ring can rotate and take different conformations, depending on the values of the respective C−C−O−H or O−C−O−H dihedral angles. As is usually the case, staggered rotamers, *trans* (t), *gauche*− (g^-) and *gauche*+ (g^+) dominate. As we will show further in the paper, conformational preferences of exocyclic hydroxyl groups influence permeation of different sugars through membranes. Details about the notation used to describe structures of monosaccharides can be found in Rao et al.[22]

Measured population of different forms of ribose, arabinose, and xylose in water[40] are listed in Table 1. All of these compounds exist preferentially in the pyranose form. Only ribose has an appreciable population (∼20%) of the furanose form. In NMR experiments it has been shown that xylose and arabinose exist mostly in $^4C_1$ and $^1C_4$ chair conformations, respectively, whereas there is some interconversion between $^4C_1$ and $^1C_4$ chair forms in ribose.[41,42] In a later NMR study[43] it was established that the dominant conformation of β-ribopyranose is $^4C_1$ chair with a small contribution (∼25%) of $^1C_4$ chair. These preferences can be explained by assigning instability factors to different ring conformations of pyranose sugars using the Reeves−Kelly scheme.[44,45] This

(28) Hénin, J.; Chipot, C. *J. Chem. Phys.* **2004**, *121*, 2904.
(29) Darve, E.; Pohorille, A. *J. Chem. Phys.* **2001**, *115*, 9169.
(30) Darve, E.; Rodríguez-Gómez, D.; Pohorille, A. *J. Chem. Phys.* **2008**, *128*, 144120.
(31) Hénin, J.; Pohorille, A.; Chipot, C. *J. Am. Chem. Soc.* **2005**, *127*, 8478.
(32) Hénin, J.; Schulten, K.; Chipot, C. *J. Phys. Chem. B* **2006**, *110*, 16718.
(33) Ivanov, I.; Cheng, X.; Sine, S. M.; McCammon, J. A. *J. Am. Chem. Soc.* **2007**, *129*, 8217.
(34) Kuang, Z.; Mahankali, U.; Beck, T. L. *Proteins: Struct., Funct., Bioinf.* **2007**, *68*, 26.
(35) Chipot, C. *Methods Mol. Biol.* **2008**, *443*, 121.
(36) Hénin, J.; Tajkhorshid, E.; Schulten, K.; Chipot, C. *Biophys. J.* **2008**, *94*, 832.
(37) Rodriguez-Gomez, D.; Darve, E.; Pohorille, A. *J. Chem. Phys.* **2004**, *120*, 3563.
(38) Straatsma, T. P.; Berendsen, H. J. C.; Stam, A. J. *Mol. Phys.* **1986**, *57*, 89.
(39) Haworth, W. N. *The Constitution of Sugars*; Edward Arnold & Co.: London, 1929.
(40) The composition of reducing sugars in solution. In *Advances in Carbohydrate Chemistry and Biochemistry*; Angyal S., Tipson, R. S., Horton, D., Eds.; Academic Press: New York, 1984; Vol. 42.
(41) Lemieux, R. U.; Stevens, J. D. *Can. J. Chem.* **1966**, *44*, 249.
(42) Rudrum, M.; Shaw, D. F. *J. Chem. Soc.* **1965**, 52.
(43) Franks, F.; Lillford, P. J.; Robinson, G. *J. Chem. Soc., Faraday Trans. 1* **1989**, *85*, 2417.
(44) Reeves, R. E. *J. Am. Chem. Soc.* **1950**, *72*, 1499.
(45) Reeves, R. E. *Adv. Carbohydr. Chem.* **1951**, *6*, 107.

Table 2. Calculated Free Energies of Transferring Different Forms of Aldopenoses from Water to Hexadecane and Corresponding Partition Coefficients Given As $-\log P$[a]

		ΔA (kcal/mol)	$-\log P$	av $-\log P$
ribose	β-ribopyranose ($^4C_1$)	6.9 ± 0.25	4.87	5.18
	β-ribopyranose ($^1C_4$)	7.81 ± 0.25	5.51	
	α-ribopyranose ($^4C_1$)	8.49 ± 0.22	5.99	
	α-ribopyranose ($^1C_4$)	9.84 ± 0.23	*b*	
	β-ribofuranose	9.15 ± 0.22	6.45	
arabinose	β-arabinose ($^1C_4$)	9.00 ± 0.26	6.35	6.50
	β-arabinose ($^4C_1$)	7.99 ± 0.22	*b*	
	α-arabinose ($^1C_4$)	9.34 ± 0.24	6.59	
xylose	β-xylose ($^4C_1$)	7.4 ± 0.19	5.22	5.35
	α-xylose ($^4C_1$)	8.19 ± 0.23	5.78	
	α-xylose ($^1C_4$)	8.84 ± 0.22	*b*	

[a] The average partition coefficients were obtained as the ratios of sugar concentrations in all forms in the two phases. [b] Populations are too low in water to be determined experimentally and therefore log P cannot be calculated.

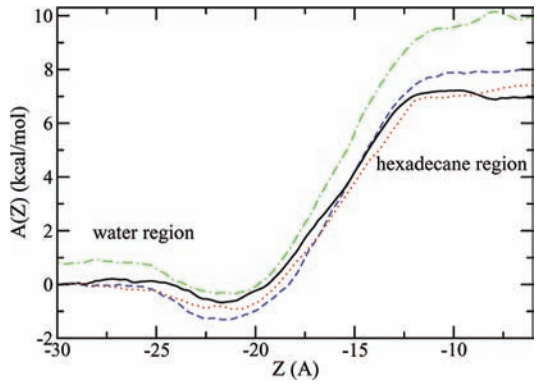

Figure 2. Free energy profiles, $A(z)$, for aldopentoses across the water−hexadecane interface obtained from ABF calculations. The solid, dotted, dashed, and dot-dashed lines are for $^4C_1$ β-ribopyranose, $^4C_1$ β-xylopyranose, $^4C_1$ β-arabinopyranose, and β-ribofuranose, respectively. $z = 0$ and $z = -30$ Å correspond to the center of the hexadecane and water lamella, respectively. The interface is located at $z = 15-20$ Å. Since only free energy differences are relevant for a given sugar, the profiles were shifted such that the free energies of the β-pyranoses in water were equal to zero.

scheme favors conformations with more hydroxyl groups in an equatorial position rather than an axial position with respect to the sugar ring. Schematic drawings of the three sugars in the conformations that are most populated in water are shown in Figure 1.

Results and Discussion

Partition Coefficients of Aldopentoses between Water and Hexadecane. For each form of ribose, arabinose, and xylose listed in Table 2 we carried out MD simulations, in which the free energy profile for transferring a sugar molecule across the water−hexadecane interface, $A(z)$, was calculated using the ABF method. Examples of such profiles are shown in Figure 2. As can be seen from this figure, $A(z)$ becomes constant at both ends of the profile, which correspond to the bulk water and hexadecane phases. The difference between these constant values, ΔA(w/h), is equal to the free energy of transferring the solute molecule from water to hexadecane. In all cases, ΔA(w/h) is positive, indicating that solubility of sugars is higher in water than in hexadecane. Between the end points $A(z)$ does not increase monotonically but instead exhibits a small minimum at the water−hexadecane interface. The origin of this minimum for neutral solutes was extensively discussed before.[46−48]

From ΔA(w/h) we can readily obtain the corresponding partition coefficient, P(w/h), which is the ratio of concentrations of the solute in two phases remaining in contact. For low solute concentrations the appropriate formula is

$$P(\text{w/h}) = \exp\left(-\frac{\Delta A(\text{w/h})}{k_B T}\right) \quad (2)$$

where T is temperature and k_B is the Boltzmann constant. The calculated values of $-\log P$(w/h) for different forms of aldopentoses are given in Table 2. Several observations can be readily made from this table. First, the lowest value of $-\log P$(w/h) was obtained for β-ribopyranose in the $^4C_1$ chair conformation. Since this is also the most populated form of ribose in water, this indicates that ribose partitions to hexadecane better than its diastereomers arabinose and xylose. Second, P(w/h) for β-ribofuranose is markedly higher than P(w/h) for β-ribopyranose. This means that the already small population of ribose in the furanoid form in water is reduced upon transfer to a nonpolar phase, so it becomes negligible. This agrees with the results of Fourier transform ion cyclotron mass spectrometry carried out for aldopentoses in the gas phase.[49] From these experiments and the accompanying quantum mechanical calculations it was estimated that the pyranose form is more stable than the furanose structure by at least 1.7 kcal/mol. A similar preference was found in quantum mechanical studies on aldohexoses.[50] Finally, assuming that hexadecane is a reasonably good proxy for the interior of the membrane, the calculated partition coefficients provide clues to answering a question: which conformations of different aldopentoses will partition most favorably into the membrane and permeate the membrane most easily? For ribose and xylose the most likely candidates are the $^4C_1$ chair conformations of β-pyranose because they have both the highest population in aqueous solution and the lowest P(w/h). Thus, these forms are selected for membrane permeability studies described in the next section.

The situation is more complicated for arabinose. The lowest partition coefficient was found for the $^4C_1$ conformation of β-pyranose, but this form of arabinose was not identified in aqueous solution in NMR experiments.[41,42] Considering that sensitivity of these experiments is 2−3%,[40,43] the $^4C_1$ conformer must be less favored in water than the $^1C_4$ chair by at least 1.5 kcal/mol. Since the difference in ΔA(w/h) between these conformers is 1 kcal/mol this implies that $^1C_4$ in hexadecane must be favored over $^4C_1$ by at least 0.5 kcal/mol. Thus the population ratio between $^1C_4$ and $^4C_1$ in this phase is at least 2.5:1. This is, however, only the lower bound, and the actual ratio might be much higher if the population of $^4C_1$ in water is less than 3%. On the basis of this estimate, it is justified to consider the $^1C_4$ rather than $^4C_1$ chair form of β-arabinopyranose in further simulations. This is consistent with quantum mechanical calculations, which predict that $^1C_4$ should be preferred over the $^4C_1$ conformation in the gas phase by 2.9 kcal/mol.[49] This comparison should be, however, taken with care because, in

(46) Pohorille, A.; Wilson, M. A. *J. Chem. Phys.* **1996**, *104*, 3760.
(47) Pohorille, A.; Wilson, M. A.; New, M. H.; Chipot, C. *Toxicol. Lett.* **1998**, *101*, 421.
(48) Pohorille, A.; New, M. H.; Schweighofer, K.; Wilson, M. A. *Curr. Top. Membr.* **1999**, *48*, 50.
(49) Guler, L. P.; Yu, Y.-Q.; Kenttämaa, H. I. *J. Phys. Chem. A* **2002**, *2106*, 6754.
(50) Lii, J.-H.; Ma, B.; Allinger, N. L. *J. Comput. Chem.* **1999**, *20*, 1594.

variance with our results, similar calculations lead to a prediction that $^1C_4$ chair should be the most stable conformation of β-ribopyranose. In general, accurate determination of conformational preferences in carbohydrates from quantum mechanical calculations is difficult because the results appear to be quite sensitive to the choice of the basis set.[50]

Another form that might contribute to permeation of arabinose through membranes is the $^1C_4$ chair conformation of α-pyranose. Its partition coefficient is somewhat larger than P(w/h) for the same conformer of β-arabinopyranose, but its population in water is also larger. Nevertheless, we will not consider it in calculating permeabilities. The consequences of this simplification will be discussed at the end of the next section.

The differences in P(w/h) for ribose and its diastereomers found in our simulations are in contrast with predictions of the partition coefficients between water and octanol using a group-additive method and the LOGKOW database.[51] These predictions yielded $-\log P$ of 2.81 for ribose and 2.91 for arabinose and xylose, which are similar to the values obtained from similar calculations by Sacerdote and Szostak (2.16 for ribose and 2.20 for arabinose and xylose).[3] The nearly identical partition coefficients for all aldopentoses led to a conclusion that differences in the free energies of transfer from water to a hydrophobic phase could not be responsible for the observed differences in the permeation rates of these sugars through membranes.[3] The discrepancy between predictions from simple models and the results of MD simulations is hardly surprising because, in contrast to atomistic simulations, group-additive methods do not account for subtle, specific solvent effects, especially if they affect intramolecular interactions in sugars. As we will argue further in the paper, these effects are likely to play an important role in determining permeabilities of membranes to different sugars. The similarity between the partition coefficients predicted from simple models is at variance not only with the results of our simulations but also with experiments on sugars in the water−octanol system, which yield a lower value of $-\log P$ for ribose than for arabinose (2.32 vs. 3.02).[52] The calculated partition coefficients in the water−hexadecane system averaged over sugar concentrations in all forms exhibit the same qualitative behavior, but are higher and the difference between ribose and arabinose is larger (see Table 2). These quantitative differences in log P between octanol and hexadecane are precisely what one might expect because octanol is more polar than hexadecane.

Permeability of POPC Membrane to Aldopentoses. Permeability of a membrane to a solute, P_m, can be well described using a model in which it is assumed that a solute molecule diffuses through the membrane in a potential defined by the free energy profile, $A(z)$, in the z-direction perpendicular to the water−membrane interface. These assumptions yield the following formula for P_m:[53]

$$\frac{1}{P_m} = \int_{z_1}^{z_2} \frac{e^{A(z)/k_BT}}{D_z(z)}\,dz \qquad (3)$$

where $D_z(z)$ is position-dependent diffusion coefficient of the molecule along z, and the limits of integration, z_1 and z_2, are located at the water−membrane interfaces. From this equation it follows that calculating permeability requires the knowledge of free energy and diffusion coefficient as functions of position along z in the full range of interest.

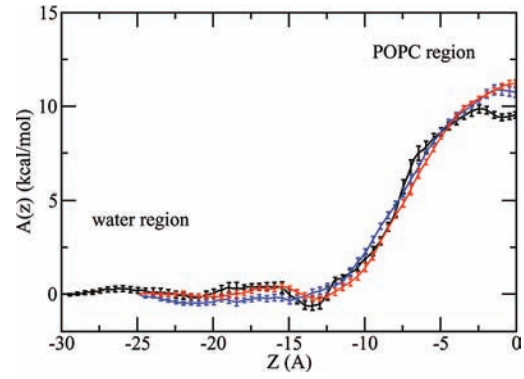

Figure 3. Free energy profile, $A(z)$, across the POPC bilayer for β-ribopyranose in the $^4C_1$ conformation (black line), β-arabinopyranose in the $^1C_4$ conformation (red line), and β-xylopyranose in the $^4C_1$ conformation (blue line). Error bars are standard errors estimated from eq 1. $z = 0$ corresponds to the center of the bilayer.

The free energy profiles for β-ribopyranose, β-arabinopyranose, and β-xylopyranose were calculated from MD simulations using the ABF method, as described in the Methods section. The simulations were carried out in the region of z that extended from bulk water ($z = -30$ Å) to the center of the bilayer ($z = 0$ Å). The other half of the free energy profile was considered to be the mirror image of the calculated $A(z)$ with respect to the $z = 0$ plane. The calculated profiles for the three sugars are shown in Figure 3. In each case $A(z)$ was set to zero in the bulk water phase. The profiles are fairly similar in water and in the outer part of the membrane but differ in the center of the bilayer. The free energy of transferring a solute from bulk water to the center of the bilayer, ΔA(w/b), is the lowest for ribose and is equal to 9.5 ± 0.2 kcal/mol. For arabinose and xylose, ΔA(w/b) is equal to 11.8 ± 0.1 and 10.9 ± 0.3 kcal/mol, respectively. All of these values are higher than the respective ΔA(w/h), indicating that partitioning of all three sugars from water to the center of the POPC bilayer is less favorable than that from water to hexadecane. However, the order of ΔA is the same in both cases and the differences in ΔA(w/b) between different sugars are quite similar to the respective differences in ΔA(w/h). This supports our assumption that the water−hexadecane system is a good model for assessing how different sugars partition between water and a phospholipids membrane. A similar conclusion was reached for partitioning of a wide range of anesthetics across water−oil and water−membrane interfaces.[46−48] In addition to the β-pyranose forms of aldopentoses, we also studied β-ribofuranose and found that ΔA(w/b) for this form is equal to 16.4 kcal/mol, i.e., it is markedly higher than for six-membered rings.

We note that orientations of sugar molecules change during transfer across the water−membrane interfaces. As expected, all orientations in aqueous solution are equally probable. In the interfacial region, the preferred orientation of the sugar ring is parallel to the membrane surface. In contrast, the sugar ring inside the POPC bilayer is orientated perpendicular to the interface. This orientation minimizes disruption in the bilayer structure caused by the presence of a sugar molecule.

The diffusion coefficient for solutes in membranes is position dependent because the environment is both anisotropic and heterogeneous. $D_z(z)$ can be related to the autocorrelation

(51) See online demo for KOW at http://srcinc.com/what-we-do/free-demos.aspx.
(52) Hansch, C.; Leo, A.; Hoekman, D. *Exploring QSAR: Hydrophobic, Electronic, and Steric Constants*; American Chemical Society: Washington, DC, 1995.
(53) Marrink, S. J.; Berendsen, H. J. C. *J. Phys. Chem.* **1994**, *98*, 4155.

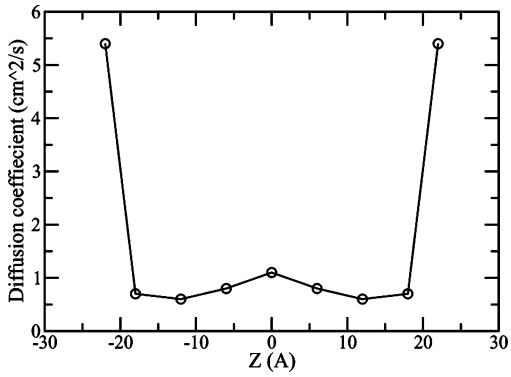

Figure 4. Calculated diffusion coefficients for the $^4C_1$ chair form of β-ribopyranose (circles). Values for $z > 0$ were obtained by assuming symmetry, $D_z(z) = D_z(-z)$.

function of random force through the fluctuation−dissipation theorem:[54]

$$D_z(z) = \frac{(k_B T)^2}{\int_0^\infty \langle \delta F_r(z,t) \delta F_r(z,0) \rangle \, dt} \quad (4)$$

Here $\delta F_r(z,t)$ is random force acting on a molecule along the z direction at time t. This random force was obtained from simulations in which the center mass of the solute was constrained to the x,y-plane at a fixed value of z. The integral of the force−force autocorrelation function for sugar molecules in bulk water converges in only 5−7 ps. The convergence is equally convincing but slower for the solute in the center of the bilayer and is reached after 60−70 ps. At the interfacial region the force−force autocorrelation function decays to zero at a very similar time scale as in the center of the bilayer, but the convergence of the integral in eq 4 is not as good. This might indicate the existence of long time scale tails in the integral that might be due to slow reorientation of the sugar in the anisotropic, interfacial environment. From the rate of convergence, we can estimate uncertainty in determining $D_z(z)$ in this region at 20−30%. As discussed further in the paper, this inaccuracy has only a minor effect on the calculated permeability coefficients. In Figure 4 we show $D_z(z)$ for β-ribopyranose calculated from eq 4. The diffusion coefficient for ribose in bulk water is equal to 5.4×10^{-6} cm^2/s, in very good agreement with the value of 6×10^{-6} cm^2/s calculated from equilibrium simulations of ribose in a box of pure water using the Einstein relation. The diffusion coefficient decreases to 0.6×10^{-6} cm^2/s at the water−POPC interface and then increases again to 1.1×10^{-6} cm^2/s at the center of the POPC membrane. Similar changes of the diffusion coefficient with the solute position in the membrane were observed previously.[53,55] We did not carry out similar simulations for xylose and arabinose. Instead we assumed that $D_z(z)$ for these sugars are very similar to that for ribose.

Once we have calculated $A(z)$ and $D_z(z)$ we can estimate the permeability of the POPC membrane to the selected sugars using eq 3. To carry out the numerical integration, the limits of integration, z_1, z_2, were set to −22 and 22 Å, and D_z was interpolated between the calculated values (see Figure 4). The integration yielded P_m equal to 81×10^{-8}, 16×10^{-8}, and 9.6×10^{-8} cm/s for ribose, arabinose, and xylose, respectively. These values are only for β-anomers of pyranoses, whereas the sugars of interest exist in water as mixtures of α- and β-anomers, with an additional, non-negligible population of the furanose form for ribose (see Table 1). Equilibration between these forms occurs at time scales (∼1000 s,[56−58]) many orders of magnitude slower than the time (∼100 ns) needed for a sugar molecule to permeate the membrane. Thus, equilibration between structural isomers or diastereomers is not likely to occur in the membrane. Since aldopentoses in the β-pyranose form have partition free energies between water and a hydrophobic oily phase lower than those of α-pyranoses and furanoses, they are expected to permeate membranes faster than other forms. Assuming that only the β-pyranose form contributes to permeability of the membrane to an aldopenose, P_m can be approximated as $P_m \approx f_\beta P_m^\beta$ (but see the discussion further in this section). Here f_β is the fraction of β-pyranose in the sugar population in water, taken from Table 1 and P_m^β is the permeability coefficient for this form. Then P_m for ribose, arabinose, and xylose is estimated at 47×10^{-8}, 5.9×10^{-8}, and 6.1×10^{-8} cm/s, respectively. These values are in very good agreement with the corresponding measured permeabilities, which are equal to 20×10^{-8}, 2.8×10^{-8}, and 2.8×10^{-8} cm/s[3]. This demonstrates that once both the sugars and the environment are considered in full atomic detail, preferential permeation of ribose can be explained using the equilibrium thermodynamics description of the behavior of a single solute. Assuming the presence of the furanose form or solute dimerization[3] is not necessary.

There are several potential sources of errors in our simulations. Of main concern is the accuracy of $A(z)$. Since $A(z)$ enters eq 3 exponentially, the calculated permeabilities are quite sensitive to the free energy barriers. Statistical accuracy, inaccuracies in the potential energy functions, slow relaxation of phospholipids, and slow rotational equilibration of exocyclic hydroxyl groups in the hydrophobic environment inside the membrane might contribute to the error in $A(z)$. To improve statistical accuracy, we increased the length of MD trajectories in the critical windows inside the bilayer to 17−25 ns. Relaxation of phospholipids is expected to be much faster than in the case of insertion of large molecules, such as peptides, into membranes because sugars do not cause massive disruptions in the membrane but instead intercalate between hydrocarbon chains. Another source of errors is the accuracy in determining $D_z(z)$. This is, however, of lesser concern because diffusion coefficient enters eq 3 linearly rather than exponentially. For this reason, approximating $D_z(z)$ for arabinose and xylose by that of ribose is not likely to influence significantly our estimates of P_m. There is also a question to what extent the model of permeation in which a solute is assumed to diffuse in the potential exerted by $A(z)$ is accurate for sugars. For small solutes nondiffusive mechanisms, such as hopping between voids in the membranes, have been implicated as contributing to solute permeation.[55,59,60] For sugar-sized, neutral solutes, however, the same mechanism is not available because these molecules cannot encounter cavities of sufficient size. This conclusion was

(54) Kubo, R. *Rep. Prog. Phys.* **1966**, *29*, 255.
(55) Marrink, S. J.; Sok, R. M.; Berendsen, H. J. C. *J. Chem. Phys.* **1996**, *104*, 9090.
(56) Acree, T. E.; Schallenberger, R. S.; Lee, Y.; Einset, J. W. *Carbohydr. Res.* **1969**, *10*, 355.
(57) Wertz, P. W.; Garver, J. C.; Anderson, L. *J. Am. Chem. Soc.* **1981**, *103*, 3916.
(58) Snyder, J. R.; Johnston, E. R.; Serianni, A. S. *J. Am. Chem. Soc.* **1989**, *111*, 2681.
(59) Lieb, W. R.; Stein, W. D. *Nature* **1969**, *224*, 240.
(60) Bassolino-Klimas, D.; Alper, H. E.; Stouch, T. R. *J. Am. Chem. Soc.* **1995**, *117*, 4118.

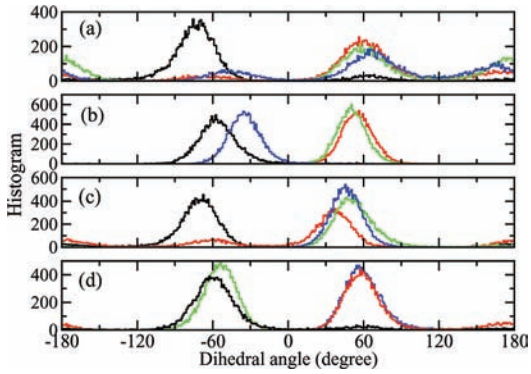

Figure 5. Population of dihedral angles $\phi_1-\phi_4$ describing rotational preferences of the four exocyclic OH groups in a sugar molecule: (a) β-ribopyranose in bulk water region, (b) β-ribopyranose in the POPC membrane, (c) β-arabinopyranose in the POPC membrane, and (d) β-xylopyranose in the POPC membrane. Black, red, green, and blue curves are for rotations of the OH_1, OH_2, OH_3, and OH_4 groups, respectively.

confirmed in simulations of drug molecules adamantane and nifedipine.[61] Thus, in our cases, the diffusion model should be appropriate.

The final concern regards the approximation that only the β-pyranose form contributes to membrane permeability. Considering the distribution of different forms of aldopentoses in solution and the results of the water−hexadecane simulations, this approximation appears to be fairly well justified for ribose and xylose. It is, however, somewhat questionable for arabinose. In this case, the α-pyranose form is slightly more populated than β-pyranose. On the other hand, the corresponding ΔA(w/h) is less favorable, but only by a few tenths of kcal/mol. Thus, α-arabinopyranose might contribute to P_m, perhaps even double its value. Fortunately, this has no negative impact on the conclusions from this work because contributions from α-pyranose would not qualitatively change the agreement between the calculated and measured permeabilities of the POPC membrane to arabinose.

Conformations of Exocyclic Hydroxyl Groups and Their Effects on Free Energy. What are the reasons for preferential permeability of membranes to ribose compared to other aldopentoses? The explanation of this effect might be related, at least in part, to rotational preferences of exocyclic groups attached to carbon atoms C_1, C_2, C_3, and C_4 of the sugar ring (for atom labeling see Figure 1). These preferences can be described by the distributions of dihedral angles O_5-C_1-O-H, C_1-C_2-O-H, C_2-C_3-O-H, and C_3-C_4-O-H. They are abbreviated $\phi_1-\phi_4$, respectively. In all cases, staggered rotamers are strongly preferred over eclipsed ones. Taking advantage of this preference we calculate populations of g^+, g^-, and t states as corresponding to $0 < \phi_i < 120°$, $-120° < \phi_i < 0°$, and $120° < \phi_i < 240°$ ($i = 1-4$), respectively. For some combinations of rotamers there is a possibility of forming electrostatically favorable O−H···O interactions between two consecutive hydroxyl groups that can be considered as distorted hydrogen bonds. For many other combinations, such a possibility does not exist.

For aldopentoses in aqueous solution, all four dihedral angles occupy most of the staggered states (see Figure 5a). This indicates the lack of strong preferences toward forming intramolecular hydrogen bonds between hydroxyl groups. This can be readily explained by observing that water molecules in the solvent have both flexibility and high affinity to form hydrogen bonds with the sugar and, therefore, effectively compete for both hydrogen bonding donors and acceptors in the exocyclic hydroxyl groups. This does not imply that all staggered rotamers are equally populated, nor does it mean that intramolecular O−H···O interactions are completely absent in aqueous solution. Instead, it means that direct or indirect (through a bridging water molecule) intramolecular O−H···O interactions are not common. A similar tendency was observed in simulations of aldohexoses in aqueous solution[62] and in NMR or infrared spectra studies on various monosaccharides.[63−65]

The situation is quite different when the sugars are located in the membrane interior. In this case, the polar, aqueous environment is replaced by nonpolar, oily chains of phospholipids, which interact with a solute only through relatively weak, nonspecific van der Waals interactions. Since water does not penetrate into this region of the bilayer, it is not available to form hydrogen bonds with the solute. In the absence of competition from water molecules, two consecutive exocyclic hydroxyl groups tend to form hydrogen bond-like interactions between themselves. These interactions are highly cooperative and lead to the formation of chains involving all four hydroxyl groups participating in three consecutive, distorted O−H···O hydrogen bonds. A similar, cooperative effect, which yielded rings of O−H···O interactions, was also found for aldohexoses in the gas phase.[49,62,66]

Since favorable intramolecular O−H···O interactions are possible only for certain combinations of ϕ angles, it follows that only a limited number of rotamers should be observed for the sugars in the membrane interior. As can be seen in Figure 5, this is indeed the case. For ribose, angles $\phi_1-\phi_4$ corresponding to g^-, g^+, g^+, and g^- rotamers, respectively, are strongly preferred. For xylose the dominant combination of rotamers is g^-, g^+, g^+, and g^-. For arabinose ϕ_1, ϕ_2, and ϕ_4 correspond to g^-, g^+ and g^+, whereas for ϕ_2 all three staggered rotamers are populated. Similar rotamer preferences have been observed for sugars in hexadecane. This indicates that these preferences are universal to nonpolar phases and suggests that the angular distributions are well converged. For ribose and xylose the preferred orientations of the hydroxyl groups correspond to chains of favorable, hydrogen bond-like interactions. The fraction of configurations in which such chains exist is 0.97 and 0.78, respectively. The chains are counterclockwise, as viewed from the β side of the ring. The same direction has been found for rings of exocyclic hydrogen bonds in aldohexoses.[66,67] For arabinose, the fraction of chains involving all four hydroxyl groups is smaller (0.21); most chains involve only two pairs and three angles: ϕ_2, ϕ_3, and ϕ_4. This is because ϕ_1 almost exclusively adopts the g^- conformation, which is not ideal for participating in chains of hydrogen bonds. A likely reason for this preference is an almost perfectly antiparallel, and therefore stabilizing, orientation of lone-pair dipoles on $O(C_1)$ and O_5. Overall, this analysis points to highly cooperative arrangements

(61) Alper, H. E.; Stouch, T. R. *J. Phys. Chem.* **1995**, *99*, 5724.
(62) Kräutler, V.; Müller, M.; Hünenberger, P. H. *Carbohydr. Res.* **2007**, *342*, 2097.
(63) Bacon, J. F.; van der Maas, J. H.; Dixon, J. R.; George, W. O.; Mclntyre, P. S. *Spectrochim. Acta, Part A* **1989**, *45*, 1313.
(64) Abraham, R. J.; Chambers, E. J.; Thomas, W. A. *J. Chem. Soc., Perkin Trans.* **1993**, *2*, 1061.
(65) de Oliveira, P. R.; Rittner, R. *Spectrochim. Acta, Part A* **2005**, *62*, 30.
(66) Ma, B.; Schaefer, H. F.; Allinger, N. L. *J. Am. Chem. Soc.* **1998**, *120*, 3411.
(67) Cramer, C. J.; Truhlar, D. G. *J. Am. Chem. Soc.* **1993**, *115*, 5745.

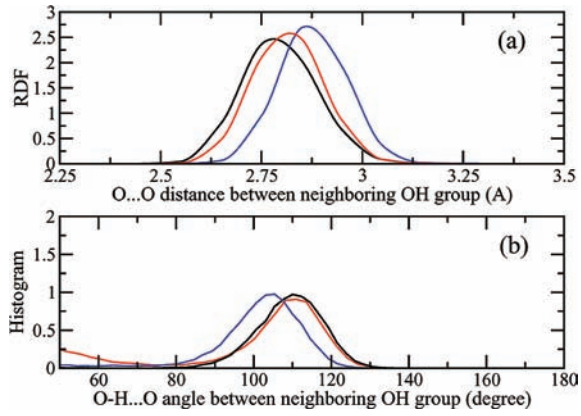

Figure 6. (a) Radial distribution function (RDF) for the O···O distance between consecutive hydroxyl groups in a sugar molecule located in the POPC bilayer, and (b) distribution of the O−H···O angle between the consecutive hydroxyl groups. Black, β-ribopyranose; red, β-arabinopyranose; blue, β-xylopyranose.

of exocyclic hydroxyl groups, which are somewhat stronger in ribose than in its diastereomers.

The average $O_i\cdots O_{i+1}$ distances vary only slightly, between 2.75 and 2.85 Å, but their distribution in ribose is somewhat shifted toward short values, compared to arabinose and xylose (see Figure 6a). In most instances, these distances are typical of conventional hydrogen bonds. This is, however, not the case for O−H···O angles. As a result of steric constraints imposed by the ring geometry, these angles are usually in the range between 90° and 120°, which makes them markedly smaller than angles found in typical hydrogen bonds. Even though this distortion implies weaker interactions, they still contribute to reducing the free energy of sugars near the center of the bilayer, thus increasing their permeation through the membrane. This effect does not appear to be equal for all three aldopentoses. If we use common geometric criteria for hydrogen bonds (O···O distance <3 Å, and O−H···O angle >120°), their averaged number per sugar configuration is 0.24 for ribose but only 0.15 and 0.03 for arabinose and xylose, respectively. If we use somewhat relaxed criteria[62] the number of hydrogen bonds per configuration increases to 1.27, 0.94, and 0.99. This suggests that intramolecular interactions between hydroxyl groups are stronger in ribose than in other aldopentoses. In contrast, a similar tendency is not seen for sugars in aqueous solution. Using the same criteria, the number of hydrogen bonds is nearly the same for all three aldopentoses and varies between 0.52 and 0.60. This means that differences in the number of effective O−H···O interactions between ribose and other aldopentoses exist only in nonpolar phases but not in water. It also supports our earlier statement that interactions between hydroxyl groups are weaker in water than in hydrophobic media. The hydrogen bonding statistics for the three sugars is collected in Table 3.

In ribose, the average values of $O_{i+1}-H_{i+1}\cdots O_i$ angles are 105°, 110°, and 114° for $i = 1, 2, 3$, respectively. These values are higher than the corresponding angles in xylose, which are all in the equatorial position and thus they are on average restricted to 103−105°. In general, as can be seen in Figure 6b, the distribution of $O_{i+1}-H_{i+1}\cdots O_i$ angles in ribose is slightly shifted toward larger values than the corresponding distributions in arabinose and xylose.

The geometric analyses of intramolecular interactions between hydroxyl groups yield a consistent picture. In nonpolar phases, such as hexadecane or the interior of a membrane, consecutive

Table 3. Averaged Number of Hydrogen Bonds per Sugar Molecule of β-Ribopyranose ($^4C_1$), β-Arabinopyranose ($^1C_4$), and β-Xylopyranose ($^4C_1$) in POPC and in Water Obtained Using Two Criteria for Defining Hydrogen Bonds

	av no. of H bond (O···O < 3.0 Å; OH···O > 120°)		av no. of H bond (O···O < 3.5 Å; OH···O> 100°)	
	in POPC	in water	in POPC	in water
ribopyranose	0.24	0.05	1.27	0.55
arabinose	0.15	0.04	0.94	0.52
xylose	0.03	0.01	0.99	0.60

O−H groups tend to form chains of energetically favorable, hydrogen bond-like interactions. Measured by distributions of $O_i\cdots O_{i+1}$ distances, values of $O_{i+1}-H_{i+1}\cdots O_i$ angles or the cooperativity in arrangements of all O−H···O pairs in a molecule, these interactions always appear stronger in ribose than in other aldopentoses. No such difference, however, is observed in water. This indicates that ribose is preferentially stabilized in nonpolar environments relative to arabinose and xylose and consequently permeates membranes faster. Whether it fully accounts for the observed differences in membrane permeabilities to ribose and its diastereomers is difficult to assess, especially since effects influencing stabilities of different forms of monosaccharides and their solvent dependence are numerous and difficult to quantify (for a review of these effects and an exhaustive list of references, see Kräutler et al.[62]). Our conclusions, however, are consistent with the findings of a quantum mechanical study on aldopentoses and several model compounds in the gas phase, in which it has been shown that hydrogen bonds influence conformational preferences considerably stronger than other factors, such as the anomeric and $\Delta 2$ effects.[49]

Relevance to the Origins of Life. The role of solute permeation in the origins of life relies on the assumption that vesicles were present on the early earth to provide barriers that separated the interior of primordial cells from the environment and to facilitate Darwinian evolution.[68] This assumption is supported by findings that under appropriate conditions amphiphilic material extracted from the Murchison meteorite or obtained in laboratory simulations of interstellar or cometary material can form vesicles.[69−71] This material contains a large fraction of fatty acids or their esters, which makes myristoleate a good model for primitive, vesicle-forming material. Although phospholipids were unlikely to be present in prebiotic milieu because no primitive biosynthetic pathways for their synthesis appear to exist, the apparent insensitivity of relative (but not absolute) permeabilities of different membranes to aldopentoses argues for the relevance of the water−POPC system in this case.

Chemical reactions inside protobiological vesicle required a supply of organic material from the environment. What the inventory of organics was that must have been delivered to primitive cells is still being debated. According to the autotrophic hypothesis, ancestors of cells produced complex organic molecules from simple substrates. In contrast, the heterotrophic model implies that protocells were able to utilize complex organics delivered from external sources. A possibility

(68) Szostak, J. W.; Bartel, D. P.; Luisi, L. P. *Nature* **2001**, *409*, 287.
(69) Deamer, D. W.; Pashley, R. M. *Origins Life Evol. Biospheres* **1989**, *19*, 21.
(70) Mautner, M.; Leonard, D.; Deamer, D. *Planet. Space Sci.* **1995**, *43*, 139.
(71) Dworkin, J.; Deamer, D.; Sandford, S.; Allamandola, L. *Proc. Nat. Acad. Sci. U.S.A.* **2001**, *98*, 815.

of sufficiently efficient and selective uptake of molecules needed to build biopolymers provides an important argument supporting the heterotrophic hypothesis.[7]

In the context of the "RNA world" hypothesis, which states that RNA molecules were the first biological polymers and acted as both catalysts of biochemical reactions and information storage systems,[72,73] the uptake of nucleotides or their building blocks, such as ribose, is of special interest. As hypothesized by Sacerdote and Szostak,[3] preferential permeation of ribose compared to other aldopentoses might have led to its selective incorporation into nucleotides, thus favoring the emergence of RNA. The results of our computer simulations support this hypothesis not only because they agree very well with experiments but also because they help to explain the observed differences in permeability coefficients at a molecular level. It should be noted, however, that integration of this hypothesis into a comprehensive scenario of protobiological chemistry is not straightforward. Despite recent progress,[74] pathways for synthesizing ribose under prebiotic conditions remain problematic. This difficulty largely motivates the search for alternatives to RNA as the first information polymers.[1,75−77] Also, preferential uptake of ribose is a strictly kinetic rather than equilibrium effect and is of significance only if the permeants are utilized in chemical reactions at rates comparable to the rates of transfer through membranes. This possibility has not yet been demonstrated in simulated prebiotic conditions. Despite these concerns, preferential permeation of ribose compared to its diastereomers is a novel mechanism that gives selective advantage to molecules of life and, therefore, is of inherent interest to protobiology.

(72) Gilbert, W. *Nature* **1986**, *319*, 618.
(73) *The RNA World*; Gestland, R. F., Cech, T. R., Atkins, J. F, Eds.; Cold Spring Harbor Laboratory Press: Cold Spring Harbor, NY, 1999.
(74) Ricardo, A.; Carrigan, M. A.; Olcott, A. N.; Benner, S. A. *Science* **2004**, *303*, 196.
(75) Wittung, P.; Nielsen, P. E.; Buchardt, O.; Egholm, M.; Norden, B. *Nature* **1994**, *368*, 561.
(76) Eschenmoser, A. *Science* **1999**, *284*, 2118.
(77) Chen, J. J.; Cai, X.; Szostak, J. W. *J. Am. Chem. Soc.* **2009**, *131*, 2119.

Conclusion

Permeation of ribose and its two diastereomers, arabinose and xylose, through the POPC membrane has been studied using MD simulations. In excellent agreement with recent experiments,[3] it has been found that ribose permeates the membrane approximately an order of magnitude faster than the other two sugars. The observed differences in permeability coefficients can be fully accounted for by considering β-anomers of aldopentoses in the pyranoid form, with a possible, additional contribution from α-arabinopyranose. It has been unnecessary to postulate that ribose exists in the membrane in the furanose form or as α-pyranose dimers, as has been previously proposed.[3] Differences in membrane permeability to aldopentoses can be explained, at least in part, by the chains of favorable, hydrogen bond-like interactions between pairs of consecutive exocyclic hydroxyl groups, which very often form in the membrane interior but only rarely in water. These interactions appear to be the strongest in ribose, thus providing increased stability in and faster permeation through the membranes, relative to other aldopentoses. In accord with the venerable Overton rule, partition coefficients between water and an oily phase are reasonably good predictors of membrane permeability to aldopentoses. Our results support a hypothesis[3] that, in the absence of sophisticated mechanisms available to contemporary organisms for achieving selectivity during synthesis and transmembrane transport, preferential uptake of ribose by primitive cells might have provided a kinetic mechanism that favored its selective incorporation into nucleic acids.

Acknowledgment. This work was supported by the NASA Exobiology Program. NASA Advanced Supercomputing (NAS) Division provided computational resources needed to carry out this study. The authors thank Michael Wilson for helpful comments.

JA902531K